Mechanical de-tethering technique for Silicon MEMS etched with DRIE process.

David Hériban, Joël Agnus, Valérie Pétrini, Michaël Gauthier

Mechanical de-tethering technique for Silicon MEMS etched with DRIE process

D Hériban

Femto-ST Institute, CNRS-UFC-ENSMM-UTBM, AS2M department, 24 rue Alain Savary, 25000 Besançon, France, EU

E-mail: david.heriban@ens2m.fr

J Agnus

Femto-ST Institute, CNRS-UFC-ENSMM-UTBM, AS2M department, 24 rue Alain Savary, 25000 Besançon, France, EU

E-mail: joel.agnus@ens2m.fr

V Petrini

Femto-ST Institute, CNRS-UFC-ENSMM-UTBM, MN2S department, 32 avenue de l'Observatoire, 25044 Besançon, France, EU

E-mail: valerie.petrini@femto-st.fr

M Gauthier

Femto-ST Institute, CNRS-UFC-ENSMM-UTBM, AS2M department, 24 rue Alain Savary, 25000 Besançon, France, EU

E-mail: michael.gauthier@femto-st.fr

Abstract.

Getting Micro-Electro-Mechanical Systems (MEMS) out of a wafer after fabrication processes is of great interest in testing, packaging or simply using these devices. Actual solutions require special machines like wafer dicing machines, increasing time and cost of de-tethering MEMS. This article deals with a new solution for manufacturing mechanical de-tetherable silicon MEMS. The presented solution could be done with DRIE process, already used in silicon MEMS fabrication, without additional time or cost. We are proposing a new way to create a notch on tethers linking both wafer and millimetric MEMS, especially designed to break with a specified mechanical force. A theoretical silicon fracture study, the experimental results and dimensional rules to design the tethers are presented in this article. This new technique is particularly useful for microscopic MEMS parts, and will find applications in the field of the MEMS components micro-assembly.

1. Introduction

Most of MEMS are manufactured into or onto single crystal silicon wafers. This kind of substrate is commonly used in microelectronics and a lot of fabrication processes are available to etch silicon. After fabrication, MEMS are localized on the wafer and they often need to be tested, packaged and used separately. A de-tethering process is then necessary. MEMS can be sized from 0.01 mm^2 to 100 mm^2, with a thickness between 50 μm and 500 μm and etched from both bulk silicon and SOI‡ wafers. These parameters include a large amount of MEMS types. Different methods are thus used in microfabrication to detach microsystems from the fabrication substrate.

The first possible method consists in dicing the wafer after fabrication to obtain freestanding MEMS. A wafer saw can be used to divide the wafer into several parts. The cutting thickness is about 200 μm and this technology is only adapted to large MEMS. Laser cutting is also used for precise application: laser spot diameter can be smaller than 10 μm. But this process requires a special and expensive machine.

A second generic method consists in fabricating systems on a sacrificial layer and releasing them by removing the sacrificial layer. The sacrificial layer can be built from different materials: In SOI wafers, the buried oxide layer (BOX) can be used as a sacrificial layer. Using anhydrous HF gas-phase etching with alcoholic vapor [1], the BOX can be etched between wafer's device and handle layers. The sacrificial layer can be a metallic layer deposed by sputtering, and wet etching process is able to detach microsystems [2]. A resin matrix can be molded around microsystems at the end of the process to protect them and join them to the wafer [3]. MEMS can be disjoined before going on to the assembly process in acetone etching solution. The use of a sacrificial layer has two major disadvantages: they require complex processes for their creation and destruction, and they can only detach a collection of microsystems.

The third method uses a breakable part between the microsystems and their substrate [4, 5]. This part can be built in the silicon between the systems and the wafer's frame, to be broken off when a mechanical stress is applied. This method permits to release one system in a collection but does not permit a large population of microsystems to be separated rapidly. In [6], tethers are designed as electric fuses, and de-tethering is made by applying a calibrated current micro-pulse on appropriate electric pads. This method is very interesting, however this process remains complex and requires a calibration of current versus geometric parameters.

A summary of the performances of major de-tethering techniques is shown in table 1. Mechanical tethers are interesting methods but they currently remain complex to use because the building of the tether in microfabrication requires adding several fabrication steps. We introduce a new method to build reliable tethers without including new steps of fabrication. The Deep Reaction Ionic Etching (DRIE) process is usually used to build 2,5D structures in single crystal silicon and polysilicon [7]. The introduced method uses

‡ Silicon On Insulator

		Wafer dicing	Laser cutting	Sacrificial layer	Fuse tether	Mechanical tether
Selective		No	Could be	No	Yes	Yes
Object size	10 to 100 mm^2	OK	OK	-	?	OK
	1 to 10 mm^2	OK	OK	OK	?	OK
	0.1 to 1 mm^2	-	OK	OK	OK	OK
	0.01 to 0.1 mm^2	-	OK	OK	OK	OK
Invest cost		Medium	High	Medium	Low	None
Operational cost		Medium	High	Low	Medium	Low
Time per object‡		–	– –	++	+	+

Table 1. De-tethering techniques

specificities of the DRIE process to build breakable tether with a specific notch in order to reduce the level of the force required and to improve the control of the location of the rupture. After fabrication, the release can be done manually or automatically: a tip is positioned up to the MEMS, then the tip pushes the MEMS and applies the required strain to break the silicon tether. One of the challenges is to correctly design tethers so that they break easily during the release step but also so they do not break during microfabrication processes, wafer transport and stocking.

The following section deals with the presentation of the method we put forward. The third section focuses on the mechanical modeling of the notched beams. The fourth section describes the implementation of the method in an application field and is followed by a discussion about the performances of this new method.

2. New de-tethering technique for silicon MEMS

To reduce the value of the breaking force, we chose to induce a brittle fracture in the silicion (not ductile) in order to obtain a rapid propagation of the crack without major deformation. To create a brittle tie, a notch is required on the silicon tether which joins MEMS to the substrate. As the easiest way to de-tether is applying a force normal to the wafer plane, we suggest to create a notch perpendicular to the substrate.

2.1. Notching principle for DRIE process

To perform high aspect ratio geometry, the DRIE process is commonly used in microfabrication because it allows an accurate control of the notch's depth [9]. We suggest to use a special phenomenon encountered in DRIE processes, the Aspect Ratio Dependent Etching (ARDE) (see figure 1) [10, 11]. Etching depth is dependent on

‡ Minus sign is used when de-tethering take too much time.

etching width i.e. the wider the width is to etch, the deeper the trench will be etched, as compared to other narrower trenches. This phenomenon usually disturbs the DRIE because etching depth cannot be equal for all features of various sizes on the substrate. In current processes, separate masks have to be used when the etched widths are quite different. However, the relationship between the depth of the trenches and the etching surface could be exploited to build notches on silicon wafers.

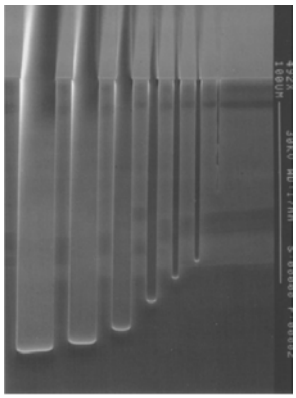

Figure 1. ARDE in silicon wafer. Side view of several DRIE trenches in silicon wafer made with different etching widths: a larger width induces a higher etching depth.

By using a very thin etching width in comparison to those used to build MEMS's structures, it is possible to create very thin notches. The major interest is to be able to build the notch in the same fabrication step as the whole structure. However the depth of the notches cannot be controlled with the same accuracy as with the regular etching process.

2.2. Flowchart

A flowchart has been defined to test our presented approach (see figure 2). The wafer used is a SOI wafer whose thicknesses are respectively 12 μm, 1 μm and 400 μm for device, buried oxide and handle layer. First, the wafer is coated with 700 nm of aluminium and 20 nm of chromium used to protect the aluminium during photoresist development. A conventional positive photoresist(MICROPOSIT 1813) is then spincoated and lithographically patterned. After photoresist's development, chromium and aluminium layers are etched and the photoresist is stripped. Having considered the experimental results obtained for ARDE with our DRIE processes, we chose a notch width of 10 μm and a width of 200μm for the etch of the MEMS' structure. The 5% ratio between both widths is able to build notches whose depth is the half of the MEMS height. The wafer is etched with a standard DRIE process until structure trenches are fully opened. The machine was a Deep RIE Alcatel A601E, with the following parameters:

- Gases: SF_6 - 300 sccm, C_4F_8 - 150 sccm
- Cycle times: SF_6 - 7 s, C_4F_8 - 2 s

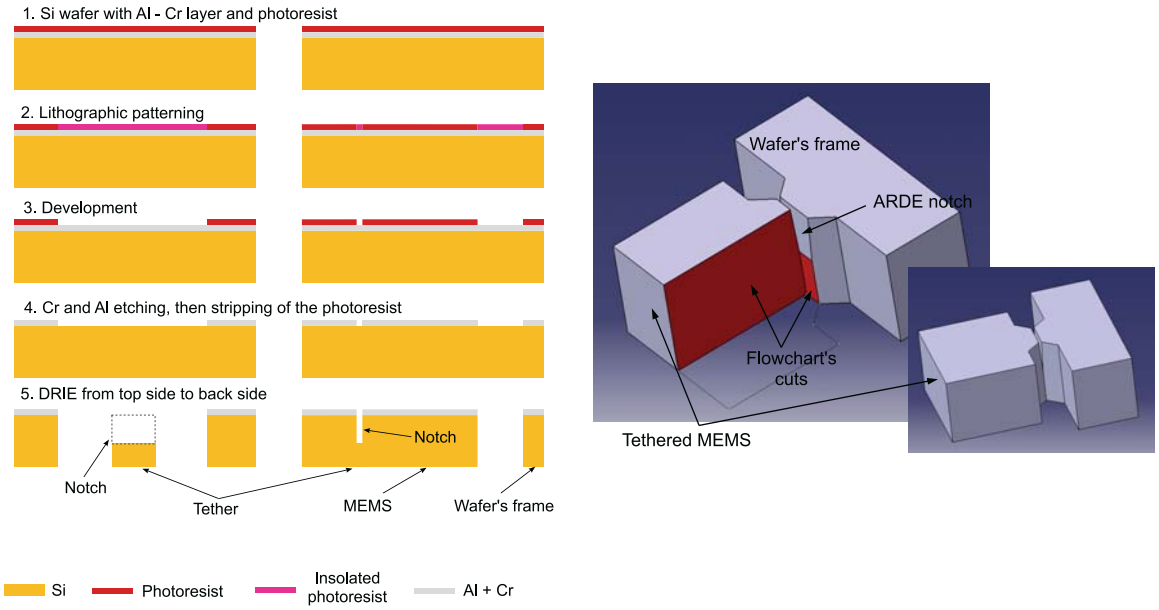

(a) Microfabrication flowchart (b) Virtual view of notched tether

Figure 2. Notch design and fabrication

- Pressure for SF_6 cycle: 4.5×10^{-2} mbar
- Temperature: 15°C
- ICP Power: 1500 W
- Bias Power: 80 W

A typical example of the experimental notches obtained with this process is presented in figure 3.

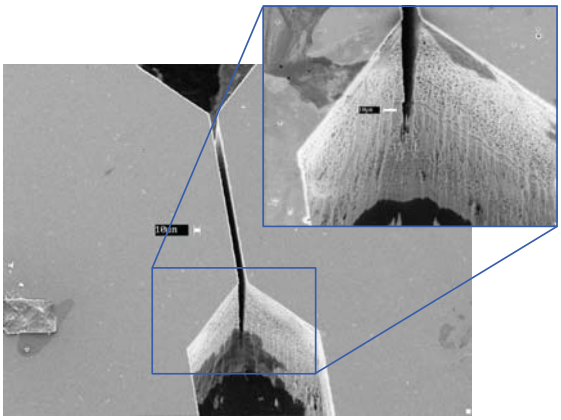

Figure 3. SEM view of notched tether

3. Generic mechanical study

A mechanical study is required to design a tether which is strong enough to hold-up during microfabrication processes and transport, but brittle enough to break without damaging MEMS during release. A mechanical model is presented to simulate the breaking force and is compared to experiments.

3.1. Mechanical modeling of notched beam under simple bending

With 1.2 GPa of yield stress (3 to 4 times greater than structural steel) single crystal silicon is a tough material but it is also very brittle. The rupture can then spread from a weak point. The notch is used to control the point where the rupture will begin and the direction of the breaking surface. Moreover, this notch enables weaker forces to be used to de-tether MEMS.

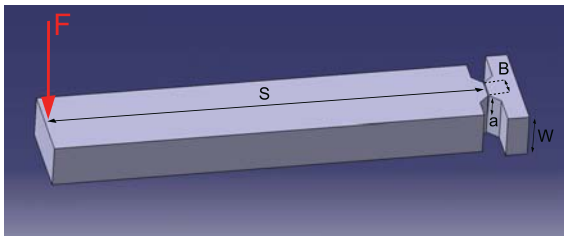

Figure 4. Geometry of notched cantilever

Many expressions of rupture behavior for materials exist in literature. In our case, the force applied to release the MEMS is normal to the substrate surface and the notched beam is thus under simple bending. In this case, a statistical expression of the force necessary to break the link is given in [12]. The model of the fracture behavior is based on the critical stress intensity factor K_{CI} which depends on beam geometry (geometric parameters S, B, a and W are shown in figure 4) and the applied force F:

$$K_{IC} = \frac{6FS}{BW^2}\frac{f_k(\alpha)}{(1-\alpha)^{3/2}}\sqrt{\pi a} \quad \text{where} \quad \alpha = \frac{a}{W} \tag{1}$$

The critical stress intensity factor is in fact proportional to the moment $F \cdot S$ applied by the force F on the notch. To obtain the breaking force for a fixed geometry with a well-known material like single crystal silicon, $f_k(\alpha)$ must be determined. Several approximated expressions are available in [13, 14] and a general value is given by [15]. Nevertheless, the expression in [12], for α values between 0.1 and 0.9, has a maximum standard deviation of 0.8% from finite element results and is precise enough for our study:

$$f_k(\alpha) = \frac{1.1215 - \alpha(1-\alpha)(0.80497 - 4.5171\alpha + 7.0374\alpha^{3/2} - 3.1383\alpha^2)}{(1+2\alpha)}$$

3.2. Critical stress intensity factor and rupture probability

The rupture probability is a function of the critical stress intensity factor and of the mechanical properties of the materials. Only experimental values are available in literature and give the rupture probability in function of the critical stress intensity factor. A complete experimental set of values, determined in function of failure probability is shown in [16] (see figure 5) on <110> plane. Most of our silicon microsystems presented in the following are made in <100> wafers. As single crystal silicon is an anisotropic material, K_{IC} values could vary in function of the crystal orientation. We first assume that the values given for <110> wafer could be extrapoled to <100> wafers. The comparison between this mechanical model and the experimental measurement is presented in the following.

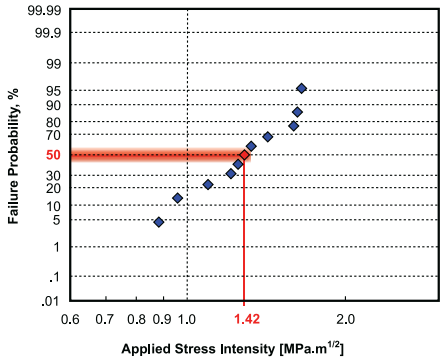

Figure 5. K_{IC} values for <110> notched single crystal silicon structures [16]

3.3. Rupture force evaluation

To determine an order of magnitude of the force required to break the link, the parameter K_{IC} for 50% of failure probability can be used:

$$K_{IC\,50\%} = 1.42\,MPa.m^{\frac{1}{2}} \tag{2}$$

Based on the equation (1), the average rupture force can be determined in relationship to the geometrical parameters and the critical stress intensity factor:

$$F = K_I \frac{BW^2(1-\alpha)^{3/2}}{6Sf_k(\alpha)\sqrt{\pi a}} \tag{3}$$

3.4. Experimental fracture force measurement

Comparing fracture model to experimental measured force requires to precisely defined the geometrical parameters and especially the depth a of the notch. The specific geometry is named "Butterfly" and is presented in figure 6. Force measurements have been done on structures where S was $1\,mm$, width B was $300\,\mu m$ and the height W of the wafer was $400\,\mu m$. Moreover, the depth of the notch a was measured after de-tethering in a Scanning Electron Microscope (see figure 7).

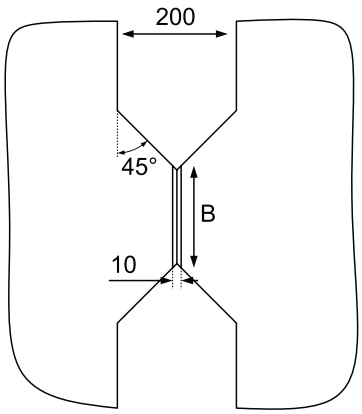

Figure 6. Geometry of the "Butterfly" tethers

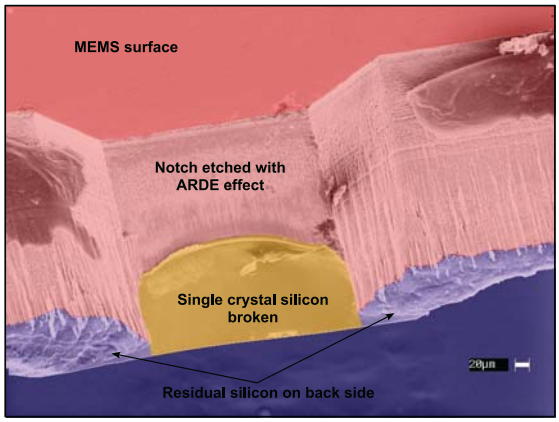

Figure 7. Colorized SEM view of de-tethered MEMS

Fracture forces have been measured on a experimental setup. A cartesian robotic structure, carrying a rigid tip (steel needle), was used up to a precision balance. This precision balance has an accuracy of 1 μN and can measure force up to 650 mN. A videomicroscope is added onto the setup to position the tip relatively to the notch with a micrometric accuracy. A force measurement curve is presented in figure 8.

Based on eight measurements of the force, rupture probabilities were calculated in relationship to the critical stress intensity factor K_{IC} defined in (1). These values were compared with the data shown in figure 5. Table 2 presents a summary of the results. Statistical data given in figure 5 and our results based on a small number of measurements are quite similar. The model we put forward could consequently be useful to design the tethers and to evaluate the average rupture forces. The study of some designs tested on experimental conditions is presented in the following section.

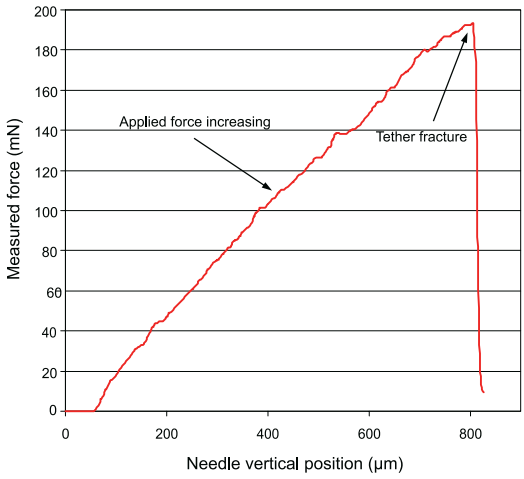

Figure 8. Force measurement during mechanical de-tethering

Force (F)) (mN)	Notch depth (a)	K_I ($MPa.m^{\frac{1}{2}}$) (μm)	Experimental rupture probability	Modeling rupture probability (fig.5)
165	220	0.97	6%	15%
218	220	1.29	19%	20%
237	220	1.40	31%	49%
243	220	1.43	44%	51%
248	220	1.46	54%	53%
252	220	1.49	69%	55%
241	230	1.55	81%	65%
258	225	1.59	94%	70%

Table 2. Rupture experimental results - 1 mm distance of the applied force

4. Example application

This section presents experimental tests on tether prototypes. Some designs of tethers were fabricated on a silicon wafer for a particular applicative context presented in the following.

4.1. Applications

The study presented in this article was applied to the manufacturing of silicon end-effectors to be mounted on a piezoelectric microgripper. Using monolythic-piezoelectric material to build the actuator and the end-effectors of a gripper greatly limits their performances. To increase gripping capabilities, we chose to glue end-effectors on the actuators (figure 9). Various gripping strategies are then possible with the same actuator. One kind of end-effector was made in a SOI wafer which has thicknesses were respectively 12 μm, 1 μm and 400 μm for device, buried oxide and handle layer [8]. The end-effectors tip is etched in the thin layer and end-effectors' base is etched in

the thick layer. The mounting process is presented in figure 11. As end-effector pairs must be glued onto the piezoelectric actuator, they require to remain aligned during the mounting process. A removable third part has then been designed to link both silicon finger tips (see figure 10). After joining, both fingers were separated by applying an appropriate force to the removable third part. This design permits end-effectors to be put easily onto the actuator and keep relative alignment of fingers.

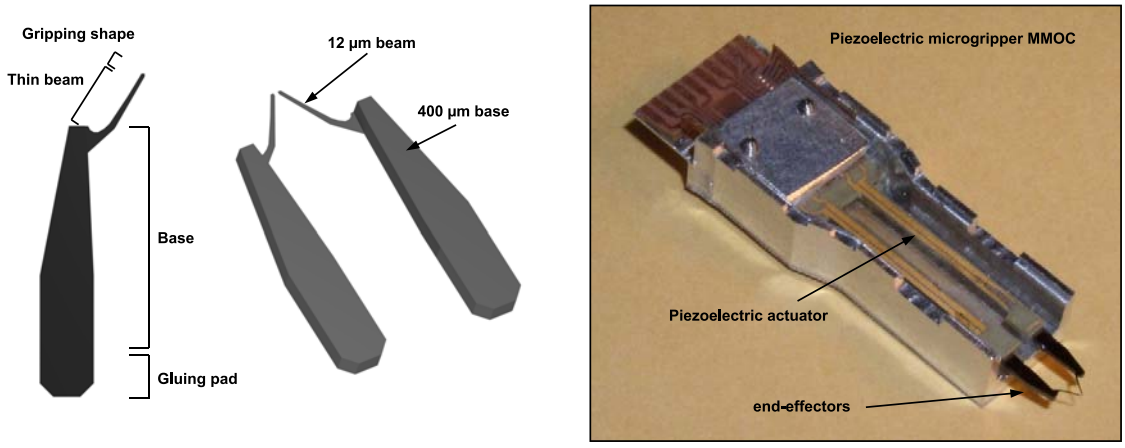

Figure 9. Silicon end effectors on the MMOC (Microprehensile Microrobot On Chip) piezoelectric microgripper.

Batch microfabrication processes are used on the whole wafer and the detachment process suggested allows to take only one end-effector pair from the others. Breakable tethers were also used for other applications like silicon micromechanical parts and microfabricated patterns for microscopic visual calibration.

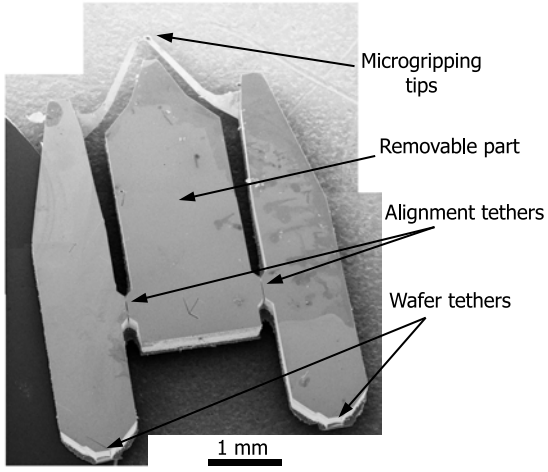

Figure 10. SEM view of the silicon end-effectors de-tethered from the wafer.

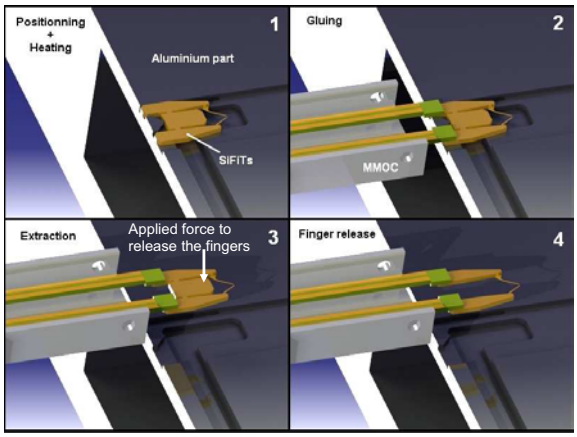

Figure 11. End-effectors SiFiTs' mounting process

4.2. Brittle tests wafer

The model of the force presented in the section below links the geometry of the tether and the force required to break it. During the design of the MEMS, the required detachment force has to be evaluated and chosen. The required force is bounded by two principles:

- firstly it has to be greater than fabrication force perturbations in order to preserve the tether during fabrication.
- Secondly the force must be smaller than the cleavage force in order to preserve the MEMS structures and the wafer's frame during rupture.

The choice of a force near to the minimum bound is sufficient, because it allows to keep structures on the wafer with a minimum damage during de-tethering. Evaluating minimum bound cannot be done in a generic way. In fact, it depends on the MEMS surface, fabrication processes, wafer thickness and condition of transportation. To evaluate it, we chose to experiment with the fabrication of different tether prototypes in classical processes (wet and dry etching, transport, clamping...). Some Butterfly structures (Btfly) presented in figure 6 have been tested using different widths B (100, 200 and 300 μm). The process shown in figure 2 was used to build notch whose depth is the half of the wafer thickness. Moreover other breakable links have been tested: straight beams whose width is 40 μm and which were notched or not. The thickness of the wafer remains 400 μm.

To perform brittle tests, 1 x 6 mm^2 beams were etched in a wafer, and each was linked by a breakable link. After the microfabrication, several tests were carried out on the wafer capacity to be manipulated and cleaved§. Results are presented in table 3. This table compares the solidity of the various tethers after each microfabrication step. 134 pairs of fingers were fabricated and tethers are presented in figure 12. The table shows that 40 μm beams are susceptible to becoming de-tethered by wet etch processes.

§ Wafer's cleavage is commonly used in microfabrication to cut the silicon dice. Silicon etched products can be then easily separate after microfabrication processes.

Tether	Notched	Initial quantity	Step 1		Step 2		Step 3		Total broken	
Btfly 100	Yes	40	1	3%	2	5%	10	25%	13	33%
Btfly 200	Yes	22	0	-	0	-	2	9%	2	9%
Btfly 300	Yes	16	0	-	0	-	0	-	0	-
Beam 40	Yes	36	8	22%	0	-	13	36%	21	58%
Beam 40	No	20	2	10%	0	-	5	25%	7	35%

Table 3. De-tethering during microfabrication steps. Step 1: dry and wet etching, Step 2: wafer's transport, Step 3: wafer's cleavage.

Liquid flows seem to cause high mechanical stress on these tethers. The wafer's cleavage brings major damages to almost whole tethers. Only massive butterfly structures of 300 μm wide stay on the wafer after all steps. The most interesting structures seem to be the butterflies 200 and 300. In our application, the Btfly 200 are in fact used to link the fingers to the wafer and Btfly 300 are used between the finger and the third removable part.

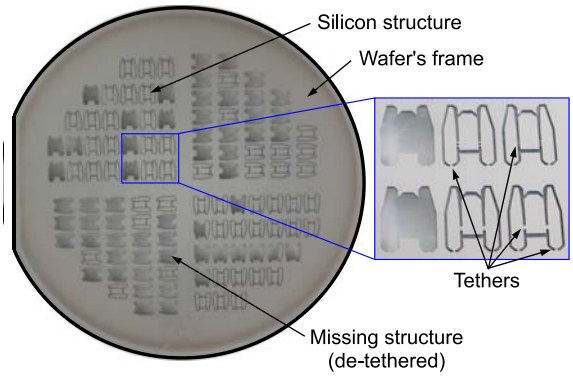

Figure 12. Experimental brittle test wafer for silicon end-effectors' design

5. Discussion

The presented detachment method is highly relevant for our application. However, this mechanical tether principle could more widely used. They have already been re-used for several millimetrical MEMS with different shapes. Theoretical model could be used for a large range of tethers and is able to estimate the force required to break the link. This section deals with different parameters which are to be taken into account to use these tethers.

5.1. Guaranteed rupture range

Minimum bound of force rupture defined in (3) cannot be estimated easily without experiments. It depends on the surface and the mass of the silicon object tethered,

microfabrication processes and stress applied to the silicon wafer. We chose to evaluate several structures in a brittle test wafer in the real fabrication process. Based on this experience, it seems necessary to test different tethers of various widths before final fabrication to verify the choice of tether geometry. Moreover, ARDE effect depends on many parameters (pressure, etched surface, mask quality, etc.) and notch depth cannot be predicted with great accuracy. Thus, a first wafer prototype could gives important information about tether geometry obtained with a specific machine.

Another solution consists in maximizing the rupture force of the tethers. With great width and small notch depth, butterfly tethers will be strong enough to endure all fabrication stress. On the other hand, rupture shock, and crack propagation may damage the silicon MEMS, as well as the wafer structure.

The rupture of tethers mainly depends on geometrical parameters, like width and the ratio between tether thickness and notch depth. The model (3) shows than the rupture moment $F \cdot S$ is proportional to the width B of the tether. Nevertheless, the influence of the notch depth a is more complex. The model (3) has been used simulate the influence of the notch depth between 0.1 and 0.9 for notch ratio. Figure 13 shows its influence on moment rupture $F \cdot S$ for fixed K_{IC} and on K_{IC} for fixed applied moment $F \cdot S$.

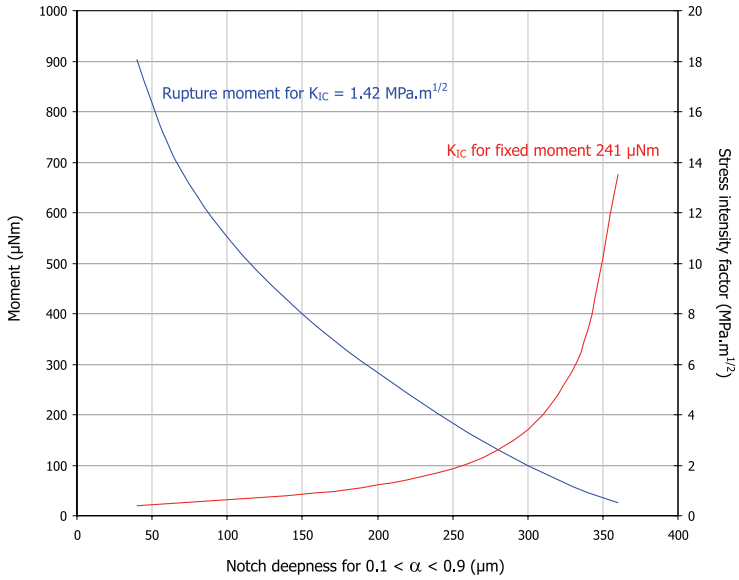

Figure 13. Influence of notch depth on theoretical model

These curves show that beyond 240 μm (eg. notch ratio of 0.6), mechanical behaviour cannot be considered as linear. Thus ARDE effect has to be bounded to this ratio, otherwise a small variation of ARDE effect could create a high variation of maximum rupture moment.

5.2. Scale effect on notched tethers

The aim of this part is to discuss the miniaturization of our method. The typical size of the microsystems tested is typically in the order of several millimeters. Our de-tethering method could be applied on microsystems whose surface is typically between 1 mm^2 to 100 mm^2. Under the millimeter square and for smaller thickness, mechanical tethers have to be redesigned.

In fact, perturbation forces are significantly reduced for micro-scaled objects. As stress forces are mainly surfacic and volumic, they decrease faster than the dimensional scale. Inertia which could induce dethethering during microfabrication process is a volumic effect and decreases rapidly with the scale. In this manner, scale effect is interesting for mechanical tethers.

Micro-objects under typical size of 100 μm require smaller tethers, and thinner etching trenches for the DRIE process. For millimetrical objects, trenches of 200 μm are commonly used for few hundred of microns etch depth. Then 10 μm trench is sufficient to open an half deep notch. When 10 μm or even 1 μm are used for etching trenches, ARDE ratio of 1:20 requires submicrometric notch trenches. And this is very difficult to obtain with regular microfabrication processes like metal-photoresist photolithography. Works are in progress to use e-beam photolithography processes to create submicrometric trenches.

5.3. Methods for de-tethering MEMS

The main goal of this paper is to present notched tether for MEMS de-tethering. However the method used to break the tether is almost as important. A force has to be applied onto the object perpendicularly to the wafer plane. But the most important is to grasp the de-tethered object during and after the release. The force applied and the rupture shock could eject the object far from its initial position. In fact, the smaller the object is, the smaller is its inertia and consequently the further it could jump [17]. For millimetrical MEMS, as our end-effectors, the rupture force can be applied manually with a tweezer and the object stays in its initial position. But for micrometrical objects, specific methods are required to not loss the objects:

- A vacuum gripper could be used to catch the object before the rupture and to apply the rupture force. As the rupture force has to be applied perpendicularly to the wafer plane, our tethers are adapted to vacuum gripping. Thus rupture does not disturb the gripping. Other axis direction for rupture should make it impossible to use a vacuum gripper.
- In the same way, a two fingered microgripper could detach and grasp the object after the rupture. A great dexterity and blocking force are used to ensure object releasing.
- The simplest method is to use a soft adhesive material to de-tether and maintain the object. A specific stamp, with an adhesive surface could be placed in contact

with the object. When the stamp is moved, the glued object is de-tethered and the softness of the adhesive material reduces the rupture shock. In function of the design of the stamp, one or several objects could be de-tethered at the same time. Object release from the stamp could be done by use of regular microgrippers.

6. Conclusion

MEMS are typically produced in batch processes on surface substrates. This mass production enables cost reduction and the fabrication of a large number of components. To disjoin all these components from the fabrication layer, wafer dicing is the most usual process. Nevertheless, for smaller MEMS or for more complex geometries than squares or rectangles, dicing is no longer feasible. Consequently, we have offered a new method to detach microsystems from the layer based on an innovative process that creates mechanical breakable tethers. These tethers which could be created with a regular DRIE process without additional processing steps enables the reduction in costs and complexity of the de-tethering step. Tested silicon tethers have few hundred micrometers lengths (100, 200, and 300 µm) and adaptable width (from 30 to 200 µm). They are sized to de-tether millimetrical MEMS dies from the fabrication silicon wafer. Rupture force range have been choosed especially for suggested structure (200 mN +/- 50 mN). A complete mechanical model, followed by a set of experimental measurements and tests have been shown. Then, its possible to tether and de-tether MEMS sized from 0.01 mm^2 to 100 mm^2, with a thickness between 50 µm and 500 µm and etched from both bulk silicon and SOI wafers. These parameters include a large amount of MEMS types. A discussion has been presented on scale reduction of the tethers and the different ways to de-tether MEMS from the fabrication wafer.

Acknowledgments

This work has been supported by the French National Projects PRONOMIA ANR-05-BLAN-0325 and NANOROL ANR-07-ROBO-0003.

References

[1] W Jang, C Choi, M Lee, C Jun and Y Kim 2002, *Fabrication of MEMS devices by using anhydrous HF gas-phase etching with alcoholic vapor*, in Journal of Micromechanics and Microengineering, vol. 12, pp. 297-306.

[2] M Gauthier and E Piat 2002 *Microfabrication and scale effect studies for a magnetic micromanipulation system*, in proc. of the IEEE Int. Conf. on Intelligent Robots and Systems, vol. 2, pp. 1754-59, Lausanne, Switzerland.

[3] Z Cuiy and R A Lawes 1997, *A new sacrificial layer process for the fabrication of micromechanical systems*, in Journal of Micromechanics and Microengineering, vol. 7, pp. 128-130.

[4] D O Popa, R Murthy, J Sin, M Mittal, H E Stephanou 2006, *M3-Modular Multi-Scale Assembly System for MEMS Packaging*, in proc. of IEEE/RSJ Int'l Conference on Intelligent Robots and Systems, Beijing, China.

[5] N Dechev, L Ren, W Liu, W L Cleghorn, J K Mills 2006, *Development of a 6 Degree of Freedom Robotic Micromanipulator for Use in 3D MEMS Microassembly*, in Proceedings of the 2006 IEEE International Conference on Robotics and Automation, Orlando, Florida.

[6] Y-S Chiu, K-S Chang, R W Johnstone and M Parameswaran 2006, *Fuse-tethers in MEMS*, in Journal of Micromechanics and Microengineering, vol. 16, pp. 480-486.

[7] Photonic MEMS Devices: Design, Fabrication and Control, by Ai-Qun Liu, CRC Press, ISBN: 9781420045680, April 2008.

[8] J Agnus, D Heriban, V Petrini and M Gauthier 2008, *Silicon End-Effectors For Microgripping Tasks* submitted to Precision Engineering.

[9] A Liu 2008, *Optical and Photonic Mems Devices - Design Fabrication and Control*, Chapter 9 *Deep Etching Fabrication Process*, pp. 353-392, CRC Press.

[10] J Yeom, Y Wu, M A Shannon 2003, *Critical aspect ratio dependence in deep reactive ion etching of silicon*, in Proceedings of the 2003 IEEE International Conference on Transducers, Solid-State Sensors, Actuators and Microsystems, vol.2, pp. 1631-1634.

[11] S H G Teo, A Q Liu, J Singh, M B Yu 2007, *Hole-type two-dimensional photonic crystal fabricated in silicon on insulator wafers*, in Sensors and Actuators A: Physical, vol.133, pp. 388-394.

[12] AD Bakker 1995, *Evaluation of elastic fracture mechanics parameters for bend specimens*, in International Journal of Fracture, vol. 71, pp. 323-343.

[13] H Tada, P C Paris, and G R Irwin 1985, *The Stress Analysis of Cracks Handbook*, Paris Productions Incorporated, St. Louis, Missouri, USA.

[14] Y Murakami 1986, *Stress Intensity Factors Handbook*, Pergamon, New York.

[15] G V Guinea, J Y Pastor, J Planas and M Elices *Stress intensity factor, compliance and CMOD for a general three-point-bend beam*, in International Journal of Fracture, vol. 89, pp. 103-116.

[16] A M Fitzgerald, R H Dauskardt, T W Kenny 2000, *Fracture toughness and crack growth phenomena of plasma-etched single crystal silicon*, Sensors and Actuators, vol. 83, pp.194-199.

[17] M Gauthier, B Lopez-Walle, C Clevy 2005, *Comparison between micro-objects manipulations in dry and liquid mediums*, in proceedings of the 2005 IEEE International Symposium on Computational Intelligence in Robotics and Automation.